3974–3987 *Nucleic Acids Research, 2007, Vol. 35, No. 12* *Published online 6 June 2007*
doi:10.1093/nar/gkm375

Effects of nucleic acid local structure and magnesium ions on minus-strand transfer mediated by the nucleic acid chaperone activity of HIV-1 nucleocapsid protein

Tiyun Wu, Susan L. Heilman-Miller and Judith G. Levin*

Section on Viral Gene Regulation, Laboratory of Molecular Genetics, National Institute of Child Health and Human Development, National Institutes of Health, Bethesda, Maryland 20892, USA

Received January 2, 2007; Revised April 27, 2007; Accepted April 30, 2007

ABSTRACT

HIV-1 nucleocapsid protein (NC) is a nucleic acid chaperone, which is required for highly specific and efficient reverse transcription. Here, we demonstrate that local structure of acceptor RNA at a potential nucleation site, rather than overall thermodynamic stability, is a critical determinant for the minus-strand transfer step (annealing of acceptor RNA to (−) strong-stop DNA followed by reverse transcriptase (RT)-catalyzed DNA extension). In our system, destabilization of a stem-loop structure at the 5′ end of the transactivation response element (TAR) in a 70-nt RNA acceptor (RNA 70) appears to be the major nucleation pathway. Using a mutational approach, we show that when the acceptor has a weak local structure, NC has little or no effect. In this case, the efficiencies of both annealing and strand transfer reactions are similar. However, when NC is required to destabilize local structure in acceptor RNA, the efficiency of annealing is significantly higher than that of strand transfer. Consistent with this result, we find that Mg^{2+} (required for RT activity) inhibits NC-catalyzed annealing. This suggests that Mg^{2+} competes with NC for binding to the nucleic acid substrates. Collectively, our findings provide new insights into the mechanism of NC-dependent and -independent minus-strand transfer.

INTRODUCTION

Human immunodeficiency virus type 1 (HIV-1) nucleocapsid protein (NC) is a small, basic, nucleic-acid-binding protein having two zinc fingers connected by a short, basic amino acid linker. Each finger contains the invariant CCHC metal-ion-binding motif (1–3). NC binds non-specifically to the phosphodiester backbone of nucleic acids (3), but also exhibits sequence-specific binding at sites with runs of Gs or T/UGs (4–10). In addition, NC is a nucleic acid chaperone and is able to catalyze nucleic acid conformational rearrangements that lead to formation of the most thermodynamically stable structures (11) (reviewed in 1–3,12). The chaperone function has two independent activities (3): aggregation of nucleic acids, localized primarily to the N-terminal basic residues (13–16); and weak destabilization of duplex molecules, associated with the zinc fingers (16–32).

The nucleic acid chaperone activity of NC is required for efficient and highly specific DNA synthesis. Indeed, NC plays an important role in almost every step in reverse transcription including the minus-strand (2,3,33) and plus-strand (9,34–38) transfer events that are mandatory for synthesis of full-length minus- and plus-strand DNAs and formation of the long-terminal repeats present at the ends of proviral DNA. In minus-strand transfer, the initial DNA product of reverse transcription, known as (−) strong-stop DNA [(−) SSDNA], is translocated to the 3′ end of the viral genome (acceptor RNA) in a reaction mediated by base pairing of the complementary repeat (R) regions at the 3′ ends of the DNA and RNA molecules (3,39).

For HIV-1, R consists of 97 nucleotides (nt). The first 59 nt in acceptor RNA and (−) SSDNA form highly stable, complementary stem-loop structures, which are referred to as transactivation response elements (TAR) RNA and TAR DNA, respectively. NC stimulates HIV-1 minus-strand transfer (3 and references therein) by transiently destabilizing the TAR structures (16,19,23–26,40–42). Destabilization of these structures promotes annealing of TAR RNA to TAR DNA (17,20,32,41,43–48) and inhibits a competing self-priming reaction at the 3′ end of (−) SSDNA (3).

*To whom correspondence should be addressed. Tel: +1 301 496 1970; Fax: +1 301 496 0243; Email: levinju@mail.nih.gov

Loop–loop interactions have been shown to be critical for dimerization and packaging of retroviral RNA (49–51) as well as for the formation of kissing complexes containing TAR RNA (52–55). Indeed, nucleation of the NC-catalyzed annealing step in minus-strand transfer was proposed to occur through interaction between the apical loops of TAR RNA and TAR DNA (56,57). However, an alternative proposal suggested that nucleation proceeds through destabilization of the 3′ and 5′ stem termini (48). Based on single-molecule FRET experiments (58) and a detailed kinetic study of NC-promoted annealing of mini-TAR constructs (32), it was also proposed that multiple pathways might be involved. More recent studies with full-length TAR suggest that a zipper mechanism involving the lower stems and bulges is the major nucleation pathway for TAR annealing in the presence of NC (59) (Vo, M.-N., Rouzina, I. and Musier-Forsyth, K., in preparation).

The structure and thermostability of the nucleic acid intermediates are major determinants for NC-facilitated minus-strand transfer. A number of studies have emphasized the importance of maintaining the bulges in the TAR DNA structure of (−) SSDNA (24–26,59–61) as well as the critical role of acceptor RNA structure (28,32,62–74). Interestingly, minus-strand transfer is more sensitive to the thermostability of acceptor RNA than to the stability and structure of (−) SSDNA (19,28). These findings are consistent with NC's weak destabilizing activity (see above) and led to the conclusion that efficient minus-strand transfer requires a delicate thermodynamic balance between the structures of (−) SSDNA and acceptor RNA and the stability of the annealed RNA–DNA hybrid (28).

In the present study, we have elucidated the paradoxical activity of two acceptor RNAs (RNA 70 and RNA 50) in minus-strand transfer: Despite the fact that RNA 70 has a higher predicted overall free energy of folding (ΔG) than RNA 50, more transfer product is synthesized with the RNA 70 acceptor than with RNA 50 in assays with the same (−) SSDNA (28). Based on extensive mutational analysis, we demonstrate for the first time that the local structure of acceptor RNA at potential nucleation sites, rather than overall thermodynamic stability, is a crucial determinant for NC chaperone activity during the minus-strand transfer step of reverse transcription.

We also show that in our reconstituted system, NC-mediated annealing is more efficient than strand transfer (i.e. annealing plus reverse transcriptase (RT)-catalyzed elongation of minus-strand DNA). Since RT activity (but not annealing) requires Mg^{2+} (75), it seemed likely that the lower values for strand transfer might be due to the presence of a high concentration of Mg^{2+} in strand transfer reactions. In fact, experiments presented below strongly suggest that Mg^{2+} competes with NC for binding to the negatively charged phosphodiester backbone in (−) SSDNA and acceptor RNA. Finally, we present data indicating that for our system, destabilization of a secondary structure formed by the 5′ TAR RNA sequence and to a lesser extent, loop–loop interactions between TAR RNA and TAR DNA contribute to efficient minus-strand transfer.

MATERIALS AND METHODS

Materials

T4 polynucleotide kinase and proteinase K were obtained from Ambion Inc. (Austin, TX, USA). [γ-^{32}P]ATP (3000 Ci/mmol) was purchased from GE Health Sciences. HIV-1 RT was obtained from Worthington. HIV-1 NC was a generous gift from Dr Robert Gorelick (SAIC Frederick, Inc., NCI-Frederick, Frederick, MD).

Methods

(−) SSDNAs. The (−) SSDNAs were synthetic DNA oligonucleotides, obtained from either Integrated DNA Technologies or Lofstrand. The 50-nt (−) SSDNA (DNA 50) is oligo JL526 (Table 1; Figure 2B). The DNA 50 compensatory mutant (JL 722) has two base changes (C17,18T) (Table 1). (−) SSDNAs were 5′-end labeled using T4 polynucleotide kinase and [γ-^{32}P]-ATP (3000 Ci/mmol), as described previously (76).

RNA preparation. Synthesis of RNA 50 and RNA 70 has been described (28). All RNA 50 and RNA 70 mutant acceptor RNAs used in this study were produced by *in vitro* transcription of a set of DNA templates containing the appropriate positive-and negative-strand sequences, respectively, as listed in Table 1: JL614 and JL615, RNA 50C49U; JL616 and JL617, RNA 50G46U; JL620 and JL621, RNA 50G48U; JL596 and JL597, RNA 70U28C; JL610 and JL611, RNA 70U28,30C; JL612 and JL613, RNA 70U30C; and JL707 and JL708, RNA 70G53,54A. *In vitro* transcription was performed using the T7-MEGAshortscript kit (Ambion Inc.), according to instructions supplied by the manufacturer. RNA products were separated from unincorporated ribonucleoside triphosphates by polyacrylamide gel electrophoresis (PAGE) in a 10% denaturing gel, followed by excision of the desired band from the gel and further purification with a Microcon YM-10 or YM-30 column (Millipore).

In vitro minus-strand transfer assay. The minus-strand transfer assay was performed as described previously (28) in the absence or presence of HIV-1 NC, at concentrations specified in the legends to the figures. Reaction mixtures contained ^{32}P-labeled (–) SSDNA and acceptor RNA at a 1:1 ratio, each at a final concentration of 10 nM. RT was also present at a final concentration of 10 nM. After incubation at 37°C for the indicated times, reactions were terminated by addition of EDTA to a final concentration of 50 mM and proteinase K to a final concentration of 0.5 μg/μl, followed by heating at 65°C for 15 min. Eight microliter of formamide loading buffer (U. S. Biochemical Corp.) was then added to the mixture, and after heating at 95°C for 3 min, a 4 μl aliquot was removed and subjected to denaturing PAGE in either a 6 or 8% gel. DNA products were visualized and quantified using a PhosphorImager (GE Health Care) and ImageQuant software, as described previously (40). The percentage of strand transfer product was calculated by dividing the amount of transfer product by the total amount of transfer product plus remaining (−) SSDNA, multiplied by 100. For time-course assays, reaction

Table 1. Oligonucleotides used in this study

Name	
	Templates for RNA transcription
JL614	5′-TAA TAC GAC TCA CTA TAG GCT GCT TTT TGC CTG TAC TGG GTC TCT CTG GTT AGA CCA GAT CTG AGT C
JL615	5′-GAC TCA GAT CTG GTC TAA CCA GAG AGA CCC AGT ACA GGC AAA AAG CAG CCT ATA GTG AGT CGT ATT A
JL616	5′-TAA TAC GAC TCA CTA TAG GCT GCT TTT TGC CTG TAC TGG GTC TCT CTG GTT AGA CCA GAT CTT AGC C
JL617	5′-GGC TAA GAT CTG GTC TAA CCA GAG AGA CCC AGT ACA GGC AAA AAG CAG CCT ATA GTG AGT CGT ATT A
JL620	5′-TAA TAC GAC TCA CTA TAG GCT GCT TTT TGC CTG TAC TGG GTC TCT CTG GTT AGA CCA GAT CTG ATC C
JL621	5′-GGA TCA GAT CTG GTC TAA CCA GAG AGA CCC AGT ACA GGC AAA AAG CAG CCT ATA GTG AGT CGT ATT A
JL596	5′-TAA TAC GAC TCA CTA TAG GCT GCT TTT TGC CTG TAC TGG GTC TCC CTG GTT AGA CCA GAT CTG AGC CTG GGA GCT CTC TGG CTA ACT
JL597	5′-AGT TAG CCA GAG AGC TCC CAG GCT CAG ATC TGG TCT AAC CAG GGA GAC CCA GTA CAG GCA AAA AGC AGC CTA TAG TGA GTC GTA TTA
JL610	5′-TAA TAC GAC TCA CTA TAG GCT GCT TTT TGC CTG TAC TGG GTC TCC CCG GTT AGA CCA GAT CTG AGC CTG GGA GCT CTC TGG CTA ACT
JL611	5′-AGT TAG CCA GAG AGC TCC CAG GCT CAG ATC TGG TCT AAC CGG GGA GAC CCA GTA CAG GCA AAA AGC AGC CTA TAG TGA GTC GTA TTA
JL612	5′-TAA TAC GAC TCA CTA TAG GCT GCT TTT TGC CTG TAC TGG GTC TCT CCG GTT AGA CCA GAT CTG AGC CTG GGA GCT CTC TGG CTA ACT
JL613	5′-AGT TAG CCA GAG AGC TCC CAG GCT CAG ATC TGG TCT AAC CGG AGA GAC CCA GTA CAG GCA AAA AGC AGC CTA TAG TGA GTC GTA TTA
JL707	5′-TAA TAC GAC TCA CTA TAG GCT GCT TTT TGC CTG TAC TGG GTC TCT CTG GTT AGA CCA GAT CTG AGC CTG AAA GCT CTC TGG CTA ACT
JL708	5′-AGT TAG CCA GAG AGC TTT CAG GCT CAG ATC TGG TCT AAC CAG AGA GAC CCA GTA CAG GCA AAA AGC AGC CTA TAG TGA GTC GTA TTA
	(−) SSDNA sequences
JL526	5′-AGT TAG CCA GAG AGC TCC CAG GCT CAG ATC TGG TCT AAC CAG AGA GAC CC
JL722	5′-AGT TAG CCA GAG AGC TTT CAG GCT CAG ATC TGG TCT AAC CAG AGA GAC CC

mixtures were scaled up and 10 µl aliquots were removed at the indicated times. The data for strand transfer and annealing (see below) represent the average of results obtained in at least three independent experiments.

Annealing assay. ^{32}P-labeled DNA 50 (WT or mutant) (0.2 pmol, final concentration 10 nM) was incubated at 37°C with 0.2 pmol (final concentration 10 nM) of acceptor RNA 70 (WT or mutants) in a final volume of 20 µl. Reactions were carried out in the absence or presence of NC in buffer containing 50 mM Tris-HCl (pH 8.0) and 75 mM KCl. The reaction mixture was scaled up as needed and 10 µl aliquots were removed at the indicated times. The labeled DNA–RNA hybrid was separated from unannealed DNA 50 by PAGE in a 6% native polyacrylamide gel (acrylamide:bis-acrylamide, 19:1) (20). The amounts of unannealed and annealed DNAs were determined by PhosphorImager analysis. To calculate the percentage of annealed DNA, the amount of annealed DNA was divided by the total amount of annealed plus unannealed DNA, multiplied by 100.

RESULTS

Secondary structures and minus-strand transfer activity of acceptor RNAs 70 and 50

In a previous study of NC chaperone activity and minus-strand transfer (28), a series of acceptor RNAs truncated in U3, the 3′ region of R, and TAR, were assayed with (−) SSDNAs having comparable truncations in complementary sequences, except that a portion of U5 rather than U3 was deleted. In general, in assays with the same DNA, acceptor RNAs with low predicted free energies of folding had more strand transfer activity than more highly structured acceptors. However, we found one striking exception when two acceptor RNAs, RNA 70 and RNA 50, were assayed with the DNA 50 (−) SSDNA (see below). To determine whether this finding could lead to new insights regarding the mechanism of nucleic acid chaperone activity in minus-strand transfer, we used the model system illustrated in Figure 1. The figure shows annealing of RNA 70 (A) or RNA 50 (B) to DNA 50 as well as the 20-nt U3 RNA sequence, which serves as the template for RT-catalyzed extension of DNA 50 to a 70-nt product.

We have now confirmed the original observations and show the data in Figure 2, for ease in following the experiments presented below. The predicted overall thermodynamic stability of RNA 70 (ΔG, −22.9 kcal/mol) is significantly higher than the predicted stability of RNA 50 (ΔG, −14.9 kcal/mol) (Figure 2A) (77,78). Yet when these RNAs were each assayed with DNA 50 (Figure 2B), RNA 70 exhibited a much higher level of strand transfer activity than RNA 50 (Figure 2C). In addition, NC had very little effect on RNA 70 activity (Figure 2C).

In an attempt to understand this result, we note that the DNA–RNA hybrid formed by RNA 70 has 50 bases complementary to DNA 50 and is therefore more stable

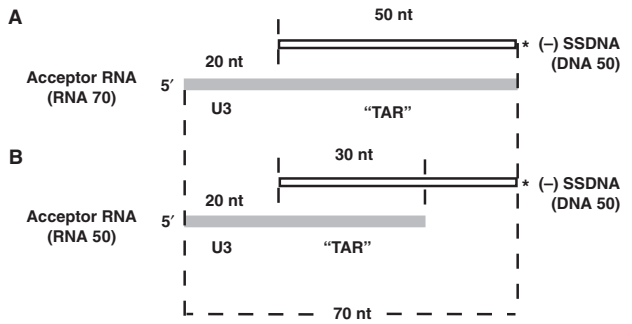

Figure 1. Schematic diagram illustrating the strand transfer system used for this study. (**A**) RNA 70. The diagram shows annealing of the 50 complementary bases in the RNA 70 acceptor and the (–) SSDNA, DNA 50, which is labeled at its 5′ end with ^{32}P. The 20 nt sequence from U3 serves as the template for RT-catalyzed DNA extension. (**B**) RNA 50. The only difference between (A) and (B) is that the RNA 50 acceptor contains only 30 nt complementary to DNA 50. With both acceptors, the final product is a 70-nt labeled DNA (dashed lines at the bottom of the figure). For RNA 70, the 'TAR' sequence is 50 nt; 9 nt at the 3′ end of full-length TAR are missing (28). RNA 50 'TAR' consists of the 5′ half of TAR (28). White rectangles, DNA 50; gray rectangles, acceptor RNA. The stars denote the ^{32}P label. The diagram is not drawn to scale.

than the RNA 50–DNA hybrid, which has only 30 complementary bases (Figure 1). In addition, RNA 70 and RNA 50 are folded differently, since RNA 70 has almost the entire TAR stem loop (nine bases from the 3′ end are missing), while RNA 50 has only the 5′ half of the TAR structure. Consequently, the local structures formed by their 5′ sequences (Figure 2A, boxed residues) also differ.

Examination of the DNA 50 structure (Figure 2B) shows that there is an 11-nt single-stranded region at the 3′ end. This region is likely to be the nucleation site for the annealing reaction, since it has no secondary structure that might interfere with annealing to the complementary bases at the 5′ ends of the TAR sequence in each acceptor RNA (Figure 2A). The predicted thermostabilities of the RNA 70 and RNA 50 local structures (Figure 2A, boxed residues) are very similar (77,79). However, destabilizing the respective structures to allow initial formation of the RNA–DNA hybrid has different consequences for each RNA: With opening of the local structure in RNA 70, the full complement of 11 bases becomes available for annealing to the 11-nt sequence in DNA 50. In contrast, only seven bases become available with destabilization

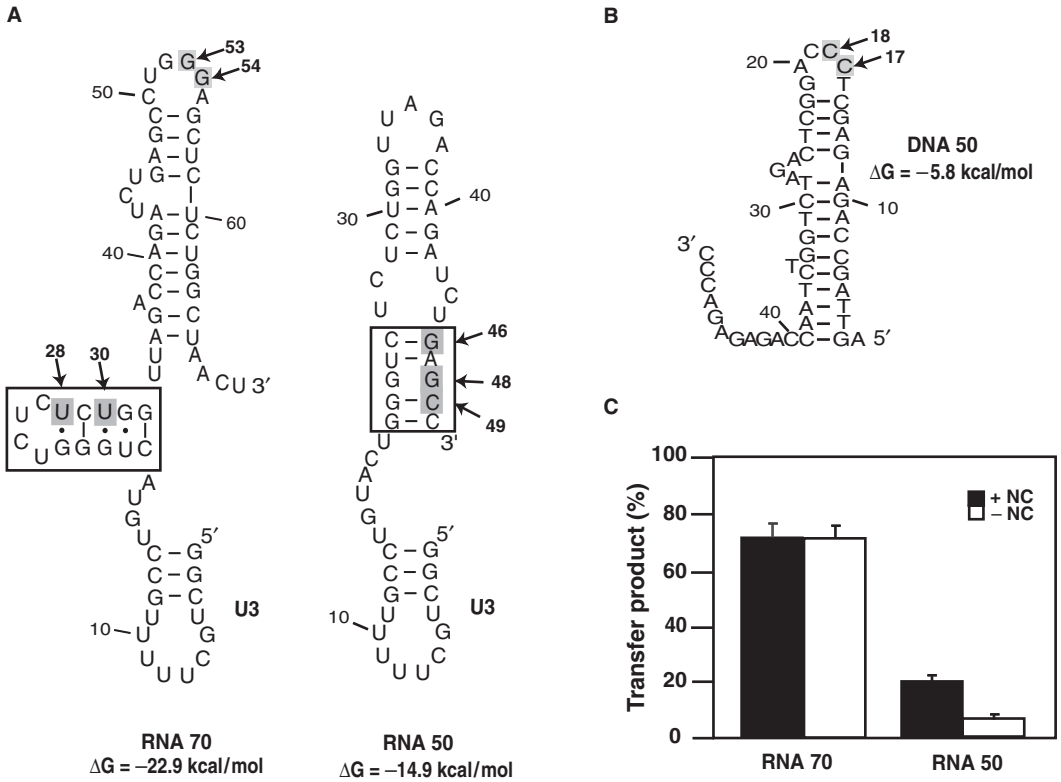

Figure 2. Influence of acceptor RNA secondary structure on minus-strand transfer. (**A**) Secondary structures of RNA 70 and RNA 50 acceptor RNAs, based on *m*Fold analysis and extensive RNase mapping studies (28). The 20-nt U3 sequences are indicated. (Note that *m*Fold predicts that two bases from U3, C19 and U20, are part of the stem-loop structure at the 5′ end of RNA 70). The predicted ΔG values are shown beneath the structures. The potential nucleation site at the 5′ end of each RNA is boxed. The arrows point to residues in RNA 70 and RNA 50 (gray shading) that were mutated. (**B**) Secondary structure of DNA 50, based on *m*Fold analysis and enzymatic mapping studies (28). The predicted ΔG value is shown on the right. The arrows indicate residues C17 and C18 (gray shading) that were mutated. Note the 11-nt single-stranded sequence at the 3′ end of the DNA. (**C**) NC-mediated minus-strand transfer. DNA 50 and RNA 70 or RNA 50 were present in reactions at a 1:1 ratio of (–) SSDNA to acceptor RNA, each with a final concentration of 10 nM. These nucleic acid concentrations were used in all of the experiments described below. Incubation was for 60 min in the absence or presence of HIV-1 NC (0.88 nt/NC), as described under the Materials and Methods section, and was followed by PAGE and PhosphorImager analysis. The bar graph shows the percentage (%) of minus-strand transfer product synthesized in each reaction. Plus NC, closed bars; minus NC, open bars.

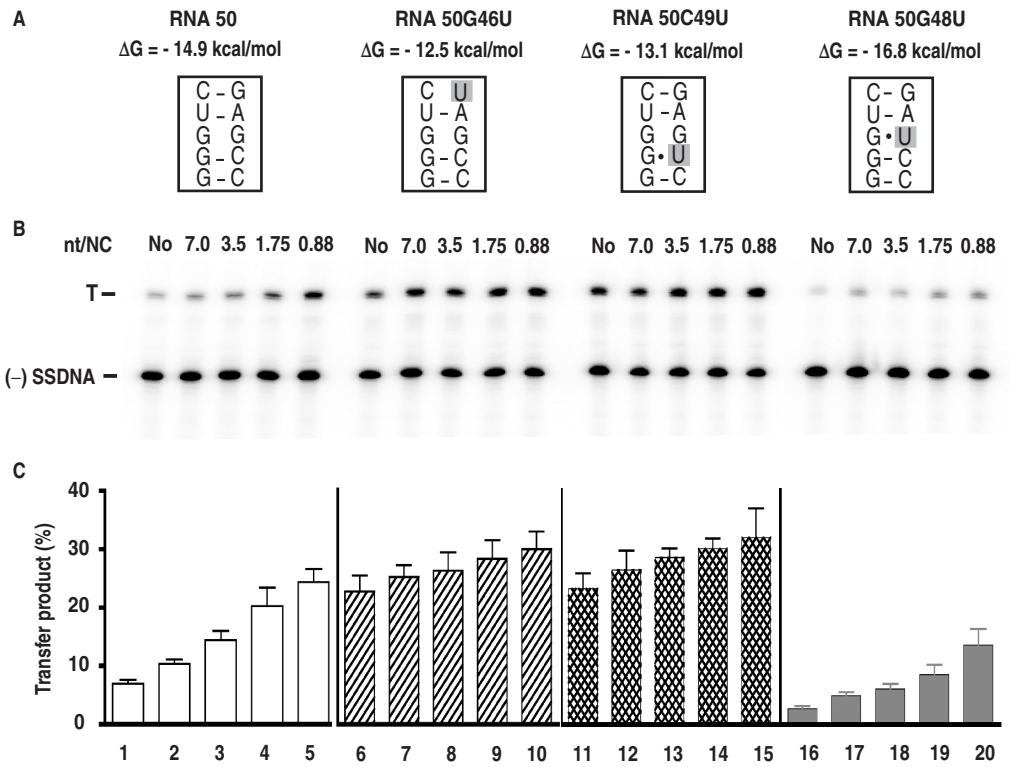

Figure 3. Effect of HIV-1 NC on minus-strand transfer with RNA 50 and RNA 50 mutants. (**A**) RNA 50 and mutants. The predicted ΔG values shown for RNA 50 and mutants represent the values for overall thermodynamic stability. The relevant sequences in each RNA are boxed. (**B**) Gel analysis. DNA 50 was incubated with acceptor RNA 50 and mutants for 60 min in the absence (No) (lanes 1, 6, 11, 16) or presence of increasing concentrations of HIV-1 NC, as follows: lanes 2, 7, 12, 17, 7 nt/NC (0.14 μM); lanes 3, 8, 13, 18, 3.5 nt/NC (0.3 μM); lanes 4, 9, 14, 19, 1.75 nt/NC (0.6 μM); lanes 5, 10, 15, 20, 0.88 nt/NC (1.2 μM). (**C**) Bar graphs showing the percentage (%) of minus-strand transfer product synthesized as a function of NC concentration. Note that the numbers below each bar in the bar graph also correspond to the lane numbers of the gel. Symbols: RNA 50, open bars; RNA 50G46U, hatched bars; RNA 50C49U, cross-hatched bars and RNA 50G48U, gray bars.

of the RNA 50 local structure. The remaining 4 nt are base paired and melting this additional stem could reduce the nucleation efficiency. This situation would account for the fact that the RNA 50 reaction is NC dependent, whereas the RNA 70 reaction is not (Figure 2C).

These considerations lead us to propose that the local structure of acceptor RNA at the nucleation site rather than overall thermodynamic stability of the entire structure is ultimately responsible for the efficiency of NC nucleic acid chaperone activity.

Effect of mutations of RNA 50 local structure on minus-strand transfer

To test this hypothesis, our strategy was to make mutations that either stabilize or destabilize the local structure of the acceptor RNAs and then to measure the effect of the mutations on minus-strand transfer. The mutations we chose were ones that retain the original RNA 50 fold (Figure 2A), thereby allowing a direct comparison of mutant and wild-type activities. Figure 3A illustrates these changes and also gives the predicted overall ΔG values for each mutant. The RNA 50 structure was destabilized in two ways: (i) by creating a mismatch (G46U); and (ii) by changing a G-C bp to a G-U wobble pair (C49U). We also made a more stable mutant of RNA 50 by changing the G-G mismatch to a G-U wobble pair (G48U). Since the RNA 50 mutants have the same fold as the wild-type (WT) RNA (data not shown), an increase or decrease in predicted ΔG values can be attributed to increased or decreased thermostability induced by the changes in local structure. Thus, mutants RNA 50G46U and RNA 50C49U (destabilizing mutations) have lower predicted ΔG values than WT RNA, while RNA 50G48U (stabilizing mutation) has a higher predicted ΔG value than WT (Figure 3A). Note that we did not make mutations in the upper stem containing the last 4 bases (nt 28–31) that are annealed to the 11 base sequence in DNA 50, since *m*FOLD analysis (77,78) revealed that most of the potential mutations in this region would result in structures that differed from RNA 50 in their overall fold.

To evaluate the behavior of the three mutated RNAs, we assayed RNA 50 and each of the RNA 50 mutants for strand transfer activity with DNA 50 (Figure 3B), as a function of increasing concentrations of HIV-1 NC (Figure 3B and C). [Note that the lane numbers for the gel (Figure 3B) are given below the individual bars in the bar graph (Figure 3C).] In contrast to RNA 70 (Figure 2C; also, see below), RNA 50 strand transfer activity was stimulated by NC in a dose-dependent manner (Figure 3B and C). At the highest concentration of NC (0.88nt/NC [1.2 μM]), stimulation was 3.5-fold

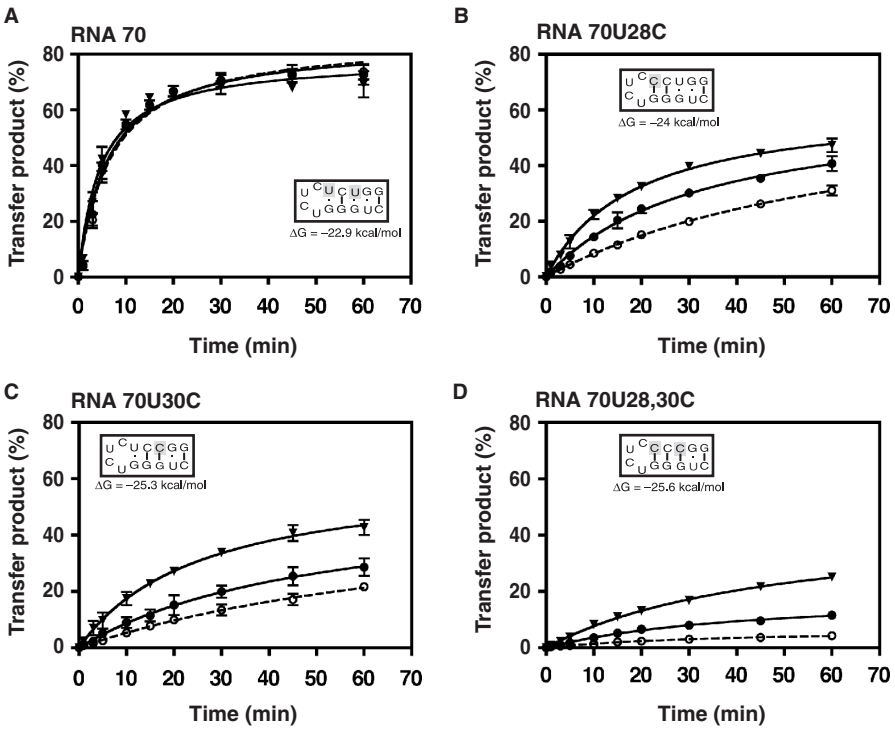

Figure 4. Kinetics of minus-strand transfer with RNA 70 and RNA 70 mutants. Reaction mixtures containing ^{32}P-labeled DNA 50 and acceptor RNA 70 (**A**), RNA 70U28C (**B**), RNA 70U30C (**C**) and RNA 70U28,30C (**D**), were incubated from 1 to 60 min without NC or with two different NC concentrations (3.5 nt/NC [0.3 μM] and 0.88 nt/NC [1.4 μM]). The percentage (%) of transfer product synthesized was plotted against time of incubation. Symbols: no NC, open circles; 3.5 nt/NC, closed circles; 0.88 nt/NC, closed inverted triangles.

(compare lanes 1 and 5). Both of the destabilizing mutants, RNA 50G46U and RNA 50C49U, showed significantly increased transfer activity in the absence of NC (lanes 6 and 11, respectively), but addition of increasing concentrations of NC resulted in only negligible stimulation of this activity (lanes 6–10 and lanes 11–15). In reactions with the stable mutant, RNA 50G48U, strand transfer activity in the absence of NC was reduced by 2.5-fold compared with that of RNA 50 (compare lane 1 with lane 16). However, NC stimulated the strand transfer activity of this mutant by 5-fold at the highest NC concentration (compare lanes 16 and 20).

Effect of mutations of RNA 70 local structure on minus-strand transfer

To further investigate whether local structure is a key determinant of NC chaperone activity, we also made three stabilizing mutations in RNA 70 (Figure 2A). It was of interest to determine the effect of these mutations on minus-strand transfer efficiency and in particular, to see whether mutant reactions would become dependent on NC concentration. Here too, our strategy was to test only mutants that have the WT RNA 70-fold. Two point mutations were constructed by changing two G-U wobble pairs to G-C base pairs (bp) (RNA 70U28C or RNA 70U30C). We also made a double mutant by changing both U28 and U30 to C (RNA 70U28,30C), thereby creating two new G-C bp to give a total of four. As expected, the RNA 70 mutants, which have increased stability of local structure, also have higher predicted overall ΔG values than WT (Figure 4, see inserts in each panel).

The time course of minus-strand transfer with acceptor RNA 70 and the three mutants was measured with DNA 50 (Figure 2B) in the presence or absence of NC (Figure 4). Examination of the end point value showed that strand transfer activity was very efficient with RNA 70 (Figures 2C and 4A). In fact, ~70% of the (−) SSDNA was converted to the transfer product at 60 min. Moreover, the extent of the reaction was independent of NC concentration (Figure 4A). However, a change of a single G-U wobble pair to a G-C bp at positions U28 or U30 (RNA 70U28C (Figure 4B) and RNA 70U30C (Figure 4C), respectively) resulted in a reduced level of activity. In the absence of NC, synthesis of the transfer product at 60 min was decreased by 3.4 (U28C)- and 2.4 (U30C)-fold compared with the end point value for RNA 70 (compare Figure 4B and C with Figure 4A). Interestingly, in both cases, NC enhanced strand transfer (by 2- and 1.5-fold, respectively, with 0.88 nt/NC [1.4 μM]) (Figure 4B and C). With the double mutant, strand transfer activity was reduced to almost background level in the absence of NC (Figure 4D). In this case, where four G-C bp need to be destabilized, NC had a relatively strong stimulatory effect, producing a 4.6-fold enhancement of the end point value with 0.88 nt/NC (Figure 4D). Despite NC stimulation of strand transfer with mutant RNA 70 acceptors, in each case the highest

Table 2A. Rates of strand transfer (k_{obs} values)[a]

RNA	Rates of strand transfer (min^{-1})		
	Minus NC	3.5 nt/NC	0.88 nt/NC
RNA 70	0.14 ± 0.010	0.15 ± 0.012	0.19 ± 0.011
RNA 70U28C	0.017 ± 0.0020	0.028 ± 0.0018	0.045 ± 0.0018
RNA 70U30C	0.020 ± 0.0013	0.040 ± 0.0026	0.058 ± 0.0023
RNA 70U28, 30C	0.030 ± 0.0033	0.029 ± 0.0022[b]	0.029 ± 0.0022[b]
RNA 70G53, 54A	0.15 ± 0.011	0.17 ± 0.012	0.19 ± 0.010
RNA 70G53, 54A-comp	0.079 ± 0.0039	0.10 ± 0.0024	0.13 ± 0.0039

[a]Rates were determined by fitting the data to a single exponential equation.
[b]Examination of the early experimental points (up to 10 min) shows NC stimulation of strand transfer beginning at 1 min and increasing with time (see text).

Table 2B. Rates of annealing (k_{obs} values)[a]

RNA	Rates of annealing (min^{-1})		
	Minus NC	3.5 nt/NC	0.88 nt/NC
RNA 70	0.15 ± 0.023	0.22 ± 0.045	0.50 ± 0.12
RNA 70U28C	0.015 ± 0.012	0.072 ± 0.0084	0.17 ± 0.0093
RNA 70U28, 30C	0.030 ± 0.018	0.054 ± 0.0054	0.10 ± 0.0089
RNA 70G53, 54A	0.061 ± 0.011	0.17 ± 0.022	0.34 ± 0.051

[a]Rates were determined by fitting the data to a single exponential equation.

level of activity at 60 min was still lower than that observed with WT RNA.

The rates of minus-strand transfer in the absence or presence of NC were also determined in reactions with each of the RNA 70 acceptors (Table 2A). With WT RNA 70, the rates were essentially the same regardless of whether NC was present (Table 2A, line 1). The rates for the two RNA 70 point mutants were dramatically reduced in the absence of NC, compared with RNA 70: 8-fold for RNA 70U28C and 7-fold for RNA 70U30C (Table 2A, first column, compare line 1 with lines 2 and 3). However, a modest stimulation of the rates (2.6 (U28C)- and 3 (U30C)-fold) was observed with increasing concentrations of NC (Table 2A, lines 2 and 3). The rate of minus-strand transfer with the double mutant was reduced to almost background level in the absence of NC (Table 2A, first column, compare lines 1 and 4). With addition of NC, there appeared to be no detectable enhancement of the initial rate (Table 2A, line 4). This could be due to the comparatively stable stem loop in the mutant structure, which NC initially might have had difficulty melting. Interestingly, when we compared the data for the early experimental time points, we found that at the highest NC concentration, the ratio of the values with and without NC increased significantly over a 10-min time interval (2.1 at 1 min; 3.3 at 3 min; ~5 at 5 min; and ~6 at 10 min) (Figure 4D). This stimulation of strand transfer was higher than that observed with the single mutants (constant ratios ~3 or 4 over 10 min).

Collectively, the data presented in Figures 3 and 4 strongly support our hypothesis that local structure at the nucleation site determines the efficiency of NC chaperone activity during minus-strand transfer. Thus, stabilizing mutations reduce strand transfer activity and increase NC dependence. Moreover, the larger the number of bp in the duplex that must be destabilized, the greater the effect of NC. In contrast, destabilizing mutations increase activity and are not greatly affected by addition of NC.

Mutation of residues in the apical loop of RNA 70 and the effect on minus-strand transfer

It was also of interest to determine whether changes in the loop residues of RNA 70 would affect strand transfer. Although RNA 70 does not have the complete 3′ stem sequence of TAR, *m*Fold analysis (data not shown) indicated that the TAR loop structure is retained (Figure 2A). We made a loop mutant by changing G53 and G54 to two A residues (see highlighted residues and arrows in Figure 2A), thereby replacing two G-C bp normally formed between bases in the RNA and DNA loops with two A-C mismatches. This mutation did not have a significant effect on the overall folding of the RNA (data not shown) and *m*Fold analysis (77,78) showed that the predicted ΔG value for the mutant (−23.4 kcal/mol) is very close to the predicted ΔG value for RNA 70 (−22.9 kcal/mol; Figure 2A).

Interestingly, like WT RNA 70, both the rate and extent of strand transfer observed with the loop mutant were not influenced by the addition of NC (Table 2A, lines 1 and 5; compare Figure 5A with Figure 4A). In reactions containing DNA 50, the rate of strand transfer with the loop mutant was the same as that with WT RNA (Table 2A, compare lines 1 and 5). Nevertheless, the end point value of the mutant reaction was reduced by almost

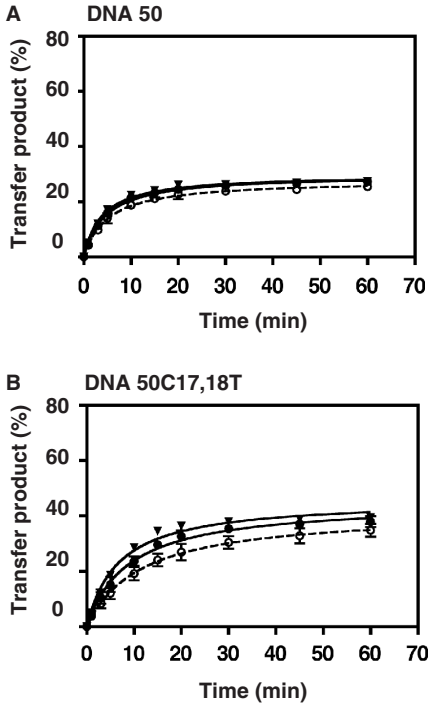

Figure 5. Kinetics of minus-strand transfer with an RNA 70 TAR loop mutant. Reaction mixtures containing the acceptor RNA 70 loop mutant and ^{32}P-labeled DNA 50 (**A**) or ^{32}P-labeled DNA 50C17,18T (a compensatory mutant) (**B**) were incubated from 1 to 60 min at 37°C without NC or with two different NC concentrations (3.5 nt/NC [0.3 μM] and 0.88 nt/NC [1.4 μM]). The percentage (%) of strand transfer product synthesized was plotted as a function of time of incubation. The symbols are described in Figure 4 legend.

3-fold (compare Figure 5A with Figure 4A), presumably due to the two mismatches in the final product. The data on the extent of strand transfer indicate that interaction of residues in the apical TAR loops in acceptor RNA and (−) SSDNA contribute to the stability of the transfer product. However, the lack of an effect on the rate suggests that the TAR loop is not the critical nucleation site in this system.

When the assay was performed with the loop mutant and a DNA 50 compensatory mutant, DNA 50C17,18T (see highlighted bases and arrows in Figure 2B), the rate was not significantly changed (Table 2A, compare lines 5 and 6). Moreover, the extent of strand transfer showed only a modest increase (~1.4-fold) compared with the value obtained with WT DNA 50 (compare Figure 5B with A). This shows that creation of two A-T bp in place of the A-C mismatches had only a small effect on increasing the stability of the final product.

Effect of local structure stability on annealing of acceptor RNA to (−) SSDNA

To gain a further understanding of the mechanism of NC chaperone activity during minus-strand transfer, it is important to know how changes in local structure affect the kinetics of annealing. The annealing reaction leads to formation of an RNA-DNA hybrid containing complementary R sequences in acceptor RNA and (-) SSDNA (3). In this study, the experiments were performed with WT RNA 70 and RNA 70 mutants (Figure 6). The results are expressed as the percentage of ^{32}P-labeled DNA 50 annealed in the reaction.

Figure 6A shows the kinetics of annealing with WT RNA 70. In contrast to the results obtained for strand transfer (Figure 4A), NC had a small stimulatory effect on annealing. Thus, the rate was increased by 3-fold with the highest concentration of NC (Table 2B, line 1), although the extent of annealing at 30 min was only minimally increased relative to the minus NC value. When the loop mutant was assayed (Figure 6B), NC significantly stimulated the rate of annealing, i.e. by 3-fold with 3.5 nt/NC (0.3 μM) and by almost 6-fold with 0.88 nt/NC (1.4 μM) (Table 2B, line 4). The end point values were 1.4- to 2-fold higher than the value for the minus NC control (Figure 6B). Thus, the annealing data for the loop mutant also differ from the strand transfer results with respect to an NC effect (Figure 5A). However, despite the stimulatory effect of NC, both the rate and extent of annealing of the loop mutant were lower than the corresponding WT values (Table 2B, compare lines 1 and 4; Figure 6A and B), most likely as a result of the two mismatches. In other experiments, we found that in reactions with the loop mutant and the DNA 50 compensatory mutant, the rate and extent of annealing were similar to the values obtained with WT DNA 50 (data not shown).

The annealing kinetics were also analyzed with the 5′ stem-loop mutants: RNA 70U28C and the double mutant RNA 70U28,30C. In the case of the single mutant, the rate of annealing was lower than that of WT, both in the absence and presence of NC (10-fold, minus NC; ~3-fold, plus NC) (Table 2B, compare lines 1 and 2). As might be expected for a more stable mutant, NC stimulated the rate of annealing to DNA 50: by 5-fold (3.5 nt/NC, 0.3 μM) and 11-fold (0.88 nt/NC,1.4 μM). In accord with our observations on the rates of annealing, the end point values were also lower than the WT values (5-fold, minus NC; ~1.4-fold, plus 3.5 nt/NC). Surprisingly, with 0.88 nt/NC, the extent of annealing was virtually the same as that of WT (compare Figure 6A and C).

With the double mutant, annealing was extremely inefficient in the absence of NC and both the rate and extent of annealing were barely detectable (Figure 6D). In the presence of NC, there was a modest increase in the rate of annealing, but the actual values at each NC concentration were ~5-fold lower than those measured for WT RNA (Table 2B, compare lines 1 and 3). Interestingly, the extent of annealing was approximately the same as that achieved by the single mutant at the highest NC concentration and here too, the value was very close to that of WT (compare Figure 6A with D).

Taken together, the data in Figure 6 and Table 2B show that for the WT and the mutants, there was a stimulatory effect of NC on annealing. This was true to a lesser extent, even for RNA 70 and the loop mutant, which did not exhibit such an effect in the strand transfer reactions (Figures 4 and 5). In addition, in the case of the stem-loop mutants whose local structures are significantly more

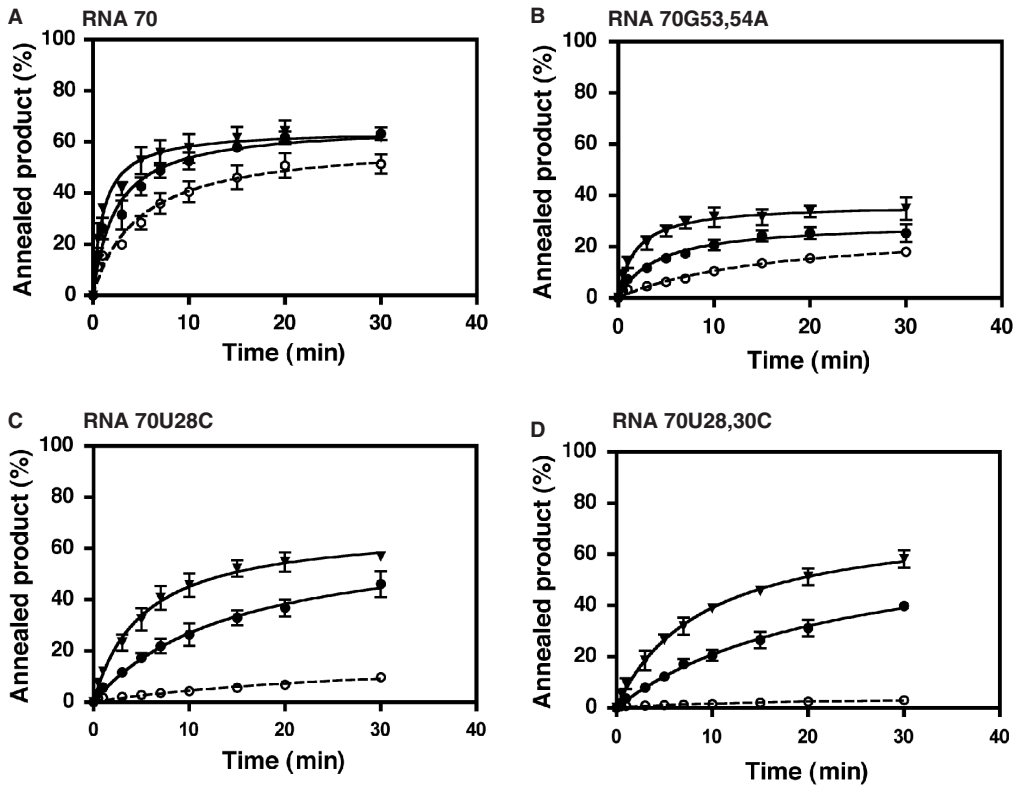

Figure 6. Annealing of RNA 70 and mutants to DNA 50. ^{32}P-labeled DNA 50 was incubated with RNA 70 (**A**), RNA 70G53,54A (**B**), RNA 70U28C (**C**) and RNA 70U28,30C (**D**) from 0.5 to 30 min at 37°C without NC or with two different NC concentrations (3.5 nt/NC [0.3 μM] and 0.88 nt/NC [1.4 μM]). The percentage (%) of DNA 50 annealed was plotted against time of incubation. Symbols are the same as those given in Figure 4 legend.

stable than that of WT RNA 70 (Figure 4), annealing was more efficient than strand transfer under our experimental conditions.

Effect of Mg^{2+} on annealing

The apparent increased efficiency of the annealing reaction with the 5′ stem-loop mutants compared with their activity in strand transfer was unexpected. We wondered whether the absence of RT, dNTPs, and 7 mM $MgCl_2$ in the annealing reaction mixtures was responsible for this result. Addition of RT or dNTPs, either singly or in combination, to annealing reactions with RNA 70, RNA 70G53,54A, or RNA 70U28,30 did not change the level of annealing (data not shown). In contrast, when increasing concentrations of Mg^{2+} were added, there was an effect on RNA–DNA hybrid formation (Figure 7).

With RNA 70, addition of 7 mM Mg^{2+} in the absence of NC (Figure 7, lane 2), NC without Mg^{2+} (lane 3) and NC plus Mg^{2+} (lanes 4–8), resulted in succeeding small, but reproducible increases in the efficiency of annealing compared with that of the minus NC reaction (lane 1). Interestingly, the stimulation observed with NC and Mg^{2+} was independent of the actual Mg^{2+} concentration (lanes 4–8). A similar pattern was observed with the RNA 70 loop mutant, except that the absolute values were reduced as a consequence of the mutation (lanes 9–16). In contrast, the double stem mutant (lanes 17–24) behaved quite differently from the other two RNA 70 acceptor RNAs. In this case, annealing activity was extremely low in the absence of NC and Mg^{2+} (lane 17) as well as in the presence of 7 mM Mg^{2+} without NC (lane 18). NC markedly stimulated annealing in the absence of Mg^{2+} (lane 19; Figure 6D), but as increasing concentrations of Mg^{2+} were added together with NC (lanes 20–24), there was a corresponding decrease in the amount of annealed product formed. At 7 mM Mg^{2+}, the reduction was ~3-fold (lane 24).

Viewed collectively, these results demonstrate that when annealing was only moderately stimulated by NC (RNA 70 and RNA 70 loop mutant), Mg^{2+} was able to increase the efficiency of the reaction without loss of the NC effect. However, when the annealing reaction was strongly dependent on NC concentration (RNA 70U28,U30C), Mg^{2+} inhibited the chaperone activity of NC. The implications of these findings are discussed below.

DISCUSSION

The goal of the present study was to provide new insights into the mechanism of HIV-1 NC nucleic acid chaperone activity in the minus-strand transfer step of reverse transcription. Our approach was to use a reconstituted system with model substrates described in an earlier report (28), since their structures are not overly complex and are therefore especially suitable for mutagenic

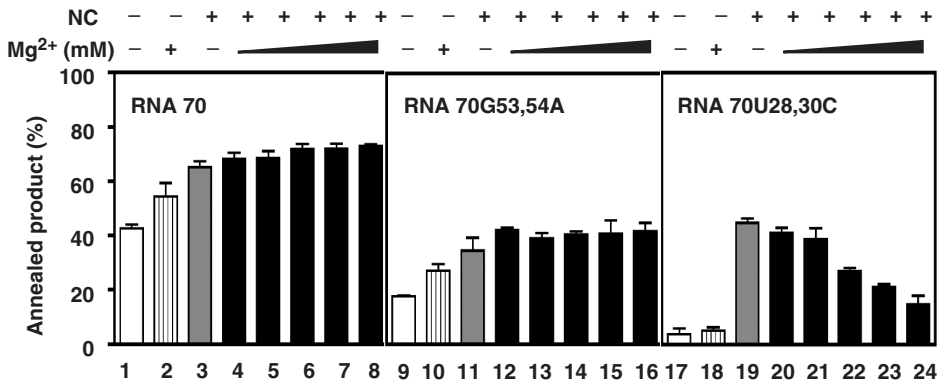

Figure 7. Effect of Mg^{2+} on annealing of RNA 70 and RNA 70 mutants to DNA 50. ^{32}P-labeled DNA 50 was incubated with RNA 70 (lanes 1–8), RNA 70G53,54A (lanes 9–16) or RNA 70U28,30C (lanes 17–24) for 30 min at 37°C under conditions indicated below. Bar graphs show the percentage (%) of DNA 50 annealed for each reaction. Symbols: open bars, no NC and no Mg^{2+} (lanes 1, 9, 17); striped bars, 7 mM Mg^{2+} alone (lanes 2, 10, 18); gray bars, 0.88 nt/NC (1.4 μM) and no Mg^{2+} (lanes 3, 11, 19); black bars, 0.88 nt/NC and increasing concentrations of Mg^{2+}as follows: 0.25 mM Mg^{2+} (lanes 4, 12, 20); 0.5 mM Mg^{2+} (lanes 5, 13, 21); 1.75 mM Mg^{2+} (lanes 6, 14, 22); 3.5 mM Mg^{2+} (lanes 7, 15, 23); 7 mM Mg^{2+} (lanes 8, 16, 24). Note that the order of addition of NC and $MgCl_2$ had no effect on the extent of annealing (data not shown).

analysis (Figure 2). We initially focused on the question of whether efficient strand transfer is determined by the overall thermodynamic stability and structure of acceptor RNA or more directly, by local structure at the nucleation site. In assays with RNA 70 and RNA 50, we found that the higher strand transfer activity exhibited by RNA 70 is correlated with the local stem-loop structure at the 5′ end of the TAR sequence, which contains 11 bases complementary to an 11-nt single-stranded region in DNA 50 (Figure 2), and *not* with RNA 70's predicted overall thermodynamic stability, which is actually considerably higher than that of RNA 50 (Figure 2A) (28).

In further support of our ideas, the data clearly demonstrated that stabilizing mutations in the relevant local structure dramatically reduce the rate and extent of strand transfer and increase dependence on NC (Figures 3 and 4), whereas destabilizing mutations lead to a marked increase in strand transfer efficiency and loss of the NC requirement (Figure 3). These results indicate that local structure at the nucleation site is a critical determinant for NC chaperone activity in minus-strand transfer. This conclusion is consistent with other studies demonstrating the importance of local structure in NC-promoted annealing of $tRNA_3^{Lys}$ to the primer-binding site in an HIV-1 RNA transcript (27), RT-catalyzed extension reactions with TAR RNA mutants (61), and HIV-1 recombination *in vivo* (69,73). Taken together with our findings, it would seem that the mechanism we have identified using a reconstituted system may also be relevant to the reverse transcription pathway utilized during the course of HIV-1 replication in infected cells.

We considered the possibility that formation of a kissing loop between the complementary TAR RNA and TAR DNA apical loops might also contribute to efficient annealing and strand transfer in our system. Previous efforts to address this question in other TAR-based systems led to diverse results. In two studies, mutational analysis showed that nucleation via loop–loop interactions facilitates efficient NC chaperone activity in minus-strand transfer (56) and annealing (57), whereas in other work, destabilization of the central double-stranded segment of the TAR stems was reported to be the major pathway for annealing, with only a minor role for a kissing-loop complex (48). Evidence has also been presented suggesting that multiple pathways may be involved in NC-dependent nucleation of annealing (32,58), although more recent studies with NC and full-length TAR favor a zipper mechanism involving the lower stems and bulges (59) (Vo,M.-N., Rouzina,I. and Musier-Forsyth,K., in preparation.)

Here we report that the major effect of mutating two of the three contiguous G residues (G53,G54) in the RNA 70 apical loop to A (Figure 2A) is an almost 3-fold reduction in the extent of strand transfer (Figures 4A and 5A). This is presumably due to the two mismatches that are created by the mutation, which results in a less stable product. A substantial effect was also observed when all three Gs were changed to A (56). Like WT RNA 70, the activity of our loop mutant is independent of NC (Figure 5A), in all likelihood because the RNA fold is unchanged by the mutation (data not shown). Making the compensatory changes in DNA 50 yields only a small improvement in the extent of strand transfer, so that the overall efficiency remains lower than that achieved with the WT substrates (Figure 5A and B). This finding implies that the loop–loop interaction must involve more than one G-C bp, since substitution of two A-T bp is not sufficient for optimal activity. Conservation of Gs in the apical loop of TAR RNA may be related to NC's preference for binding to unpaired Gs (3 and references therein) and to the unusual stability of a kissing complex, even with only two G-C bp (80,81).

It is of interest that mutations in the RNA 70 local structure at the 5′ end of TAR and in the apical loops both affect the extent of strand transfer (Figures 4 and 5). However, 'only' stabilizing mutations in the RNA 70 5′ stem loop have striking effects on 'both' the rate and extent of strand transfer and are NC dependent

(Table 2A). Thus, it appears that destabilization of the RNA 70 5′ local structure is likely to be the dominant nucleation pathway for minus-strand transfer in the RNA 70 system.

Another issue that we address concerns a comparison between annealing and strand transfer activities in the presence or absence of NC. The RNA 70 acceptors that we tested fall into two groups, i.e. having activity that is either independent (group 1) or dependent (group 2) on NC. With the RNAs in the first group (WT RNA 70 and the RNA 70 loop mutant), strand transfer is unaffected by addition of NC (Figures 4A and 5A), although NC slightly stimulates the extent of annealing (Figure 6A and B). The lower minus NC values for annealing compared with the corresponding values for strand transfer might reflect the fact that during strand transfer, RT-catalyzed elongation of the annealed DNA drives the equilibrium towards formation of a more thermodynamically stable product with a greater number of base pairs than the number contained in the RNA–DNA hybrid. When NC is present, the rate of annealing is increased (Table 2B, lines 1 and 4) so that even in the absence of RT, the end point values for annealing and strand transfer are in close agreement. The RT effect observed here is reminiscent of a somewhat similar scenario that occurs during plus-strand transfer (3): annealing of the complementary primer-binding site sequences in (+) SSDNA and minus-strand acceptor DNA is ultimately favored over hybrid formation between the 3′ terminus of $tRNA_3^{Lys}$ and (+) SSDNA, since RT extends each strand of the DNA duplex to yield the more stable double-stranded DNA transfer product (35).

RNA 70 acceptors with stabilizing changes in the 5′ local stem-loop structure, e.g. RNA 70U28C and RNA 70U28,30C (group 2), show a clear dependence on NC for efficient annealing and strand transfer (Figures 4 and 6) and a striking reduction in the rates of these reactions relative to the rates for WT RNA 70 (Table 2). In the absence of NC, the annealing and strand transfer activities of both the single and double mutants are quite low. However, in reactions with NC, the annealing activities of both mutants are greatly increased and reach a value of almost 60% at the highest NC concentration (Figure 6C and D), whereas the comparable values for strand transfer are significantly lower (Figure 4B and D). These results indicate that optimal experimental conditions for annealing and strand transfer may differ when activity is dependent on NC's chaperone function. We have reported similar findings in studies with NC mutants having changes in the CCHC motif (17,20).

To investigate this discrepancy between the efficiency of annealing and strand transfer with structured RNA acceptors, we tested annealing under strand transfer conditions. We found that of the components present specifically in strand transfer reactions, it is only Mg^{2+} that inhibits NC chaperone activity during annealing and in a dose-dependent manner (Figure 7C). This would explain why a potential stabilizing effect of Mg^{2+} on the nucleic acid substrates does not lead to greater stimulation of strand transfer by NC, as might be expected. In fact, since Mg^{2+} is present in vast excess over NC in our reactions, the data strongly suggest that Mg^{2+} successfully competes with NC for non-specific binding to the phosphodiester backbone of the nucleic acid substrates and partially displaces NC. Not surprisingly, since Mg^{2+} does not have nucleic acid chaperone activity, we observe that formation of the annealed RNA–DNA hybrid becomes very inefficient in the presence of high Mg^{2+} concentrations. This conclusion is consistent with a similar observation made by Musier-Forsyth and colleagues (32) (Vo,M.-N., Rouzina, I. and Musier-Forsyth,K., in preparation).

The Mg^{2+} concentration in virions and in infected cells is not known. However, in some instances the concentration in uninfected cells has been reported to be much lower (~0.2–0.25 mM) than the amounts typically used in reverse transcription reactions *in vitro* (6–8 mM) (75 and references therein). If the intracellular Mg^{2+} concentration in infected cells is also low, it would suggest that RT-catalyzed extension can proceed at a lower Mg^{2+} concentration *in vivo* than *in vitro* and that, under such conditions, Mg^{2+} should not interfere with the efficiency of NC-dependent annealing during HIV-1 infection. Interestingly, in reactions containing 0.25 mM Mg^{2+} and NC, we find only an ~8% reduction in annealing (Figure 7C). In reactions with WT RNA 70 and the loop mutant, which have a fairly minor requirement for NC, annealing is stimulated by Mg^{2+} to a small, but constant extent, over a wide range of Mg^{2+} concentrations (Figure 7A and B). In this case, when the ionic strength is increased, the increase in positive charge leads to greater attraction between the nucleic acid strands and results in more efficient annealing, in accord with studies on the aggregation properties of NC (10,13,14,82).

In conclusion, we have demonstrated that the local structure in acceptor RNA at the nucleation site is a critical determinant for nucleation of annealing that occurs during HIV-1 minus-strand transfer. Moreover, destabilization of a short secondary structure at the 5′ end of the TAR sequence in RNA 70 appears to be the dominant nucleation pathway. Our data also point to different consequences for annealing versus strand transfer when *in vitro* reactions are strongly or weakly dependent on NC. Where NC has little or no effect, annealing and strand transfer occur with similar efficiencies. However, when NC-catalyzed destabilization of acceptor structure is required, annealing appears to be more efficient than strand transfer. We attribute this result to the presence of a high Mg^{2+} concentration in reconstituted strand transfer reactions, which leads to a competition between Mg^{2+} and NC for binding to the negatively charged phosphate groups in the nucleic acid strands. Taken together, these findings contribute significantly to a greater understanding of the mechanism of NC nucleic acid chaperone activity during minus-strand transfer.

ACKNOWLEDGEMENTS

We are indebted to Dr Robert J. Gorelick for his generous gift of recombinant NC. We are also grateful to Drs Karin Musier-Forsyth and Ioulia Rouzina for many valuable

discussions and for providing data prior to publication. In addition, we thank Drs Musier-Forsyth, Rouzina and Alan Rein for critical reading of the manuscript. This research was supported by the Intramural Research Program of the NIH, National Institute of Child Health and Human Development. Funding to pay the Open Access publication charges for this article was provided by the Intramural Research Program of the NIH, National Institute of Child Health and Human Development.

Conflict of interest statement. None declared.

REFERENCES

1. Darlix,J.-L., Lapadat-Tapolsky,M., de Rocquigny,H. and Roques,B.P. (1995) First glimpses at structure-function relationships of the nucleocapsid protein of retroviruses. *J. Mol. Biol.*, **254**, 523–537.
2. Rein,A., Henderson,L.E. and Levin,J.G. (1998) Nucleic-acid-chaperone activity of retroviral nucleocapsid proteins: significance for viral replication. *Trends Biochem. Sci.*, **23**, 297–301.
3. Levin,J.G., Guo,J., Rouzina,I. and Musier-Forsyth,K. (2005) Nucleic acid chaperone activity of HIV-1 nucleocapsid protein: critical role in reverse transcription and molecular mechanism. *Prog. Nucleic Acid Res. Mol. Biol.*, **80**, 217–286.
4. South,T.L. and Summers,M.F. (1993) Zinc- and sequence-dependent binding to nucleic acids by the N-terminal zinc finger of the HIV-1 nucleocapsid protein: NMR structure of the complex with the Psi-site analog, dACGCC. *Protein Sci.*, **2**, 3–19.
5. De Guzman,R.N., Wu,Z.R., Stalling,C.C., Pappalardo,L., Borer,P.N. and Summers,M.F. (1998) Structure of the HIV-1 nucleocapsid protein bound to the SL3 ψ-RNA recognition element. *Science*, **279**, 384–388.
6. Fisher,R.J., Rein,A., Fivash,M., Urbaneja,M.A., Casas-Finet,J.R., Medaglia,M. and Henderson,L.E. (1998) Sequence-specific binding of human immunodeficiency virus type 1 nucleocapsid protein to short oligonucleotides. *J. Virol.*, **72**, 1902–1909.
7. Morellet,N., Déméné,H., Teilleux,V., Huynh-Dinh,T., de Rocquigny,H., Fournié-Zaluski,M.-C. and Roques,B.P. (1998) Structure of the complex between the HIV-1 nucleocapsid protein NCp7 and the single-stranded pentanucleotide d(ACGCC). *J. Mol. Biol.*, **283**, 419–434.
8. Vuilleumier,C., Bombarda,E., Morellet,N., Gérard,D., Roques,B.P. and Mély,Y. (1999) Nucleic acid sequence discrimination by the HIV-1 nucleocapsid protein NCp7: a fluorescence study. *Biochemistry*, **38**, 16816–16825.
9. Johnson,P.E., Turner,R.B., Wu,Z.R., Hairston,L., Guo,J., Levin,J.G. and Summers,M.F. (2000) A mechanism for plus-strand transfer enhancement by the HIV-1 nucleocapsid protein during reverse transcription. *Biochemistry*, **39**, 9084–9091.
10. Fisher,R.J., Fivash,M.J., Stephen,A.G., Hagan,N.A., Shenoy,S.R., Medaglia,M.V., Smith,L.R., Worthy,K.M., Simpson,J.T. *et al.* (2006) Complex interactions of HIV-1 nucleocapsid protein with oligonucleotides. *Nucleic Acids Res.*, **34**, 472–484.
11. Tsuchihashi,Z. and Brown,P.O. (1994) DNA strand exchange and selective DNA annealing promoted by the human immunodeficiency virus type 1 nucleocapsid protein. *J. Virol.*, **68**, 5863–5870.
12. Herschlag,D. (1995) RNA chaperones and the RNA folding problem. *J. Biol. Chem.*, **270**, 20871–20874.
13. Stoylov,S.P., Vuilleumier,C., Stoylova,E., De Rocquigny,H., Roques,B.P., Gérard,D. and Mély,Y. (1997) Ordered aggregation of ribonucleic acids by the human immunodeficiency virus type 1 nucleocapsid protein. *Biopolymers*, **41**, 301–312.
14. Le Cam,E., Coulaud,D., Delain,E., Petitjean,P., Roques,B.P., Gérard,D., Stoylova,E., Vuilleumier,C., Stoylov,S.P. and Mély,Y. (1998) Properties and growth mechanism of the ordered aggregation of a model RNA by the HIV-1 nucleocapsid protein: an electron microscopy investigation. *Biopolymers*, **45**, 217–229.
15. Krishnamoorthy,G., Roques,B., Darlix,J.-L. and Mély,Y. (2003) DNA condensation by the nucleocapsid protein of HIV-1: a mechanism ensuring DNA protection. *Nucleic Acids Res.*, **31**, 5425–5432.
16. Beltz,H., Clauss,C., Piémont,E., Ficheux,D., Gorelick,R.J., Roques,B., Gabus,C., Darlix,J.-L., de Rocquigny,H. *et al.* (2005) Structural determinants of HIV-1 nucleocapsid protein for cTAR DNA binding and destabilization, and correlation with inhibition of self-primed DNA synthesis. *J. Mol. Biol.*, **348**, 1113–1126.
17. Guo,J., Wu,T., Anderson,J., Kane,B.F., Johnson,D.G., Gorelick,R.J., Henderson,L.E. and Levin,J.G. (2000) Zinc finger structures in the human immunodeficiency virus type 1 nucleocapsid protein facilitate efficient minus- and plus-strand transfer. *J. Virol.*, **74**, 8980–8988.
18. Williams,M.C., Rouzina,I., Wenner,J.R., Gorelick,R.J., Musier-Forsyth,K. and Bloomfield,V.A. (2001) Mechanism for nucleic acid chaperone activity of HIV-1 nucleocapsid protein revealed by single molecule stretching. *Proc. Natl Acad. Sci. USA*, **98**, 6121–6126.
19. Bernacchi,S., Stoylov,S., Piémont,E., Ficheux,D., Roques,B.P., Darlix,J.-L. and Mély,Y. (2002) HIV-1 nucleocapsid protein activates transient melting of least stable parts of the secondary structure of TAR and its complementary sequence. *J. Mol. Biol.*, **317**, 385–399.
20. Guo,J., Wu,T., Kane,B.F., Johnson,D.G., Henderson,L.E., Gorelick,R.J. and Levin,J.G. (2002) Subtle alterations of the native zinc finger structures have dramatic effects on the nucleic acid chaperone activity of human immunodeficiency virus type 1 nucleocapsid protein. *J. Virol.*, **76**, 4370–4378.
21. Urbaneja,M.A., Wu,M., Casas-Finet,J.R. and Karpel,R.L. (2002) HIV-1 nucleocapsid protein as a nucleic acid chaperone: spectroscopic study of its helix-destabilizing properties, structural binding specificity, and annealing activity. *J. Mol. Biol.*, **318**, 749–764.
22. Williams,M.C., Gorelick,R.J. and Musier-Forsyth,K. (2002) Specific zinc-finger architecture required for HIV-1 nucleocapsid protein's nucleic acid chaperone function. *Proc. Natl Acad. Sci. USA*, **99**, 8614–8619.
23. Azoulay,J., Clamme,J.-P., Darlix,J.-L., Roques,B.P. and Mély,Y. (2003) Destabilization of the HIV-1 complementary sequence of TAR by the nucleocapsid protein through activation of conformational fluctuations. *J. Mol. Biol.*, **326**, 691–700.
24. Beltz,H., Azoulay,J., Bernacchi,S., Clamme,J.-P., Ficheux,D., Roques,B., Darlix,J.-L. and Mély,Y. (2003) Impact of the terminal bulges of HIV-1 cTAR DNA on its stability and the destabilizing activity of the nucleocapsid protein NCp7. *J. Mol. Biol.*, **328**, 95–108.
25. Beltz,H., Piémont,E., Schaub,E., Ficheux,D., Roques,B., Darlix,J.-L. and Mély,Y. (2004) Role of the structure of the top half of HIV-1 cTAR DNA on the nucleic acid destabilizing activity of the nucleocapsid protein NCp7. *J. Mol. Biol.*, **338**, 711–723.
26. Cosa,G., Harbron,E.J., Zeng,Y., Liu,H.W., O'Connor,D.B., Eta-Hosokawa,C., Musier-Forsyth,K. and Barbara,P.F. (2004) Secondary structure and secondary structure dynamics of DNA hairpins complexed with HIV-1 NC protein. *Biophys. J.*, **87**, 2759–2767.
27. Hargittai,M.R.S., Gorelick,R.J., Rouzina,I. and Musier-Forsyth,K. (2004) Mechanistic insights into the kinetics of HIV-1 nucleocapsid protein-facilitated tRNA annealing to the primer binding site. *J. Mol. Biol.*, **337**, 951–968.
28. Heilman-Miller,S.L., Wu,T. and Levin,J.G. (2004) Alteration of nucleic acid structure and stability modulates the efficiency of minus-strand transfer mediated by the HIV-1 nucleocapsid protein. *J. Biol. Chem.*, **279**, 44154–44165.
29. Kankia,B.I., Barany,G. and Musier-Forsyth,K. (2005) Unfolding of DNA quadruplexes induced by HIV-1 nucleocapsid protein. *Nucleic Acids Res.*, **33**, 4395–4403.
30. Cruceanu,M., Gorelick,R.J., Musier-Forsyth,K., Rouzina,I. and Williams,M.C. (2006) Rapid kinetics of protein-nucleic acid interaction is a major component of HIV-1 nucleocapsid protein's nucleic acid chaperone function. *J. Mol. Biol.*, **363**, 867–877.
31. Narayanan,N., Gorelick,R.J. and Destefano,J.J. (2006) Structure/Function mapping of amino acids in the N-terminal zinc finger of the human immunodeficiency virus type 1 nucleocapsid protein: residues responsible for nucleic acid helix destabilizing activity. *Biochemistry*, **45**, 12617–12628.

32. Vo,M.-N., Barany,G., Rouzina,I. and Musier-Forsyth,K. (2006) Mechanistic studies of mini-TAR RNA/DNA annealing in the absence and presence of HIV-1 nucleocapsid protein. *J. Mol. Biol.*, **363**, 244–261.
33. Cristofari,G. and Darlix,J.-L. (2002) The ubiquitous nature of RNA chaperone proteins. *Prog. Nucleic Acid Res. Mol. Biol.*, **72**, 223–268.
34. Auxilien,S., Keith,G., Le Grice,S.F.J. and Darlix,J.-L. (1999) Role of post-transcriptional modifications of primer $tRNA^{Lys,3}$ in the fidelity and efficacy of plus strand DNA transfer during HIV-1 reverse transcription. *J. Biol. Chem.*, **274**, 4412–4420.
35. Wu,T., Guo,J., Bess,J., Henderson,L.E. and Levin,J.G. (1999) Molecular requirements for human immunodeficiency virus type 1 plus-strand transfer: analysis in reconstituted and endogenous reverse transcription systems. *J. Virol.*, **73**, 4794–4805.
36. Muthuswami,R., Chen,J., Burnett,B.P., Thimmig,R.L., Janjic,N. and McHenry,C.S. (2002) The HIV plus-strand transfer reaction: determination of replication-competent intermediates and identification of a novel lentiviral element, the primer over-extension sequence. *J. Mol. Biol.*, **315**, 311–323.
37. Egelé,C., Schaub,E., Ramalanjaona,N., Piémont,E., Ficheux,D., Roques,B., Darlix,J.-L. and Mély,Y. (2004) HIV-1 nucleocapsid protein binds to the viral DNA initiation sequences and chaperones their kissing interactions. *J. Mol. Biol.*, **342**, 453–466.
38. Égelé,C., Schaub,E., Piémont,E., de Rocquigny,H. and Mély,Y. (2005) Investigation by fluorescence correlation spectroscopy of the chaperoning interactions of HIV-1 nucleocapsid protein with the viral DNA initiation sequences. *C. R. Biol.*, **328**, 1041–1051.
39. Telesnitsky,A. and Goff,S.P. (1993) Strong-stop strand transfer during reverse transcription. In Skalka,A.M. and Goff,S.P. (eds), *Reverse Transcriptase*, Cold Spring Harbor Laboratory Press, Cold Spring Harbor, NY, pp. 49–83.
40. Guo,J., Henderson,L.E., Bess,J., Kane,B. and Levin,J.G. (1997) Human immunodeficiency virus type 1 nucleocapsid protein promotes efficient strand transfer and specific viral DNA synthesis by inhibiting TAR-dependent self-priming from minus-strand strong-stop DNA. *J. Virol.*, **71**, 5178–5188.
41. Hong,M.K., Harbron,E.J., O'Connor,D.B., Guo,J., Barbara,P.F., Levin,J.G. and Musier-Forsyth,K. (2003) Nucleic acid conformational changes essential for HIV-1 nucleocapsid protein-mediated inhibition of self-priming in minus-strand transfer. *J. Mol. Biol.*, **325**, 1–10.
42. Cosa,G., Zeng,Y., Liu,H.W., Landes,C.F., Makarov,D.E., Musier-Forsyth,K. and Barbara,P.F. (2006) Evidence for non-two-state kinetics in the nucleocapsid protein chaperoned opening of DNA hairpins. *J. Phys. Chem. B Condens. Matter Mater Surf Interfaces Biophys.*, **110**, 2419–2426.
43. You,J.C. and McHenry,C.S. (1994) Human immunodeficiency virus nucleocapsid protein accelerates strand transfer of the terminally redundant sequences involved in reverse transcription. *J. Biol. Chem.*, **269**, 31491–31495.
44. Lapadat-Tapolsky,M., Pernelle,C., Borie,C. and Darlix,J.-L. (1995) Analysis of the nucleic acid annealing activities of nucleocapsid protein from HIV-1. *Nucleic Acids Res.*, **23**, 2434–2441.
45. Davis,W.R., Gabbara,S., Hupe,D. and Peliska,J.A. (1998) Actinomycin D inhibition of DNA strand transfer reactions catalyzed by HIV-1 reverse transcriptase and nucleocapsid protein. *Biochemistry*, **37**, 14213–14221.
46. Guo,J., Wu,T., Bess,J., Henderson,L.E. and Levin,J.G. (1998) Actinomycin D inhibits human immunodeficiency virus type 1 minus-strand transfer in *in vitro* and endogenous reverse transcriptase assays. *J. Virol.*, **72**, 6716–6724.
47. Golinelli,M.-P. and Hughes,S.H. (2003) Secondary structure in the nucleic acid affects the rate of HIV-1 nucleocapsid-mediated strand annealing. *Biochemistry*, **42**, 8153–8162.
48. Godet,J., de Rocquigny,H., Raja,C., Glasser,N., Ficheux,D., Darlix,J.-L. and Mély,Y. (2006) During the early phase of HIV-1 DNA synthesis, nucleocapsid protein directs hybridization of the TAR complementary sequences via the ends of their double-stranded stem. *J. Mol. Biol.*, **356**, 1180–1192.
49. Paillart,J.C., Shehu-Xhilaga,M., Marquet,R. and Mak,J. (2004) Dimerization of retroviral RNA genomes: an inseparable pair. *Nat. Rev. Microbiol.*, **2**, 461–472.
50. Russell,R.S., Liang,C. and Wainberg,M.A. (2004) Is HIV-1 RNA dimerization a prerequisite for packaging? Yes, no, probably? *Retrovirology*, **1**, 23.
51. D'Souza,V. and Summers,M.F. (2005) How retroviruses select their genomes. *Nat. Rev. Microbiol.*, **3**, 643–655.
52. Chang,K.-Y. and Tinoco,I.Jr (1994) Characterization of a "kissing" hairpin complex derived from the human immunodeficiency virus genome. *Proc. Natl Acad. Sci. USA*, **91**, 8705–8709.
53. Boiziau,C., Dausse,E., Yurchenko,L. and Toulmé,J.J. (1999) DNA aptamers selected against the HIV-1 *trans*-activation-responsive RNA element form RNA-DNA kissing complexes. *J. Biol. Chem.*, **274**, 12730–12737.
54. Collin,D., van Heijenoort,C., Boiziau,C., Toulmé,J.-J. and Guittet,E. (2000) NMR characterization of a kissing complex formed between the TAR RNA element of HIV-1 and a DNA aptamer. *Nucleic Acids Res.*, **28**, 3386–3391.
55. Nair,T.M., Myszka,D.G. and Davis,D.R. (2000) Surface plasmon resonance kinetic studies of the HIV TAR RNA kissing hairpin complex and its stabilization by 2-thiouridine modification. *Nucleic Acids Res.*, **28**, 1935–1940.
56. Berkhout,B., Vastenhouw,N.L., Klasens,B.I.F. and Huthoff,H. (2001) Structural features in the HIV-1 repeat region facilitate strand transfer during reverse transcription. *RNA*, **7**, 1097–1114.
57. Kanevsky,I., Chaminade,F., Ficheux,D., Moumen,A., Gorelick,R., Negroni,M., Darlix,J.-L. and Fossé,P. (2005) Specific interactions between HIV-1 nucleocapsid protein and the TAR element. *J. Mol. Biol.*, **348**, 1059–1077.
58. Liu,H.W., Cosa,G., Landes,C.F., Zeng,Y., Kovaleski,B.J., Mullen,D.G., Barany,G., Musier-Forsyth,K. and Barbara,P.F. (2005) Single-molecule FRET studies of important intermediates in the nucleocapsid-protein-chaperoned minus-strand transfer step in HIV-1 reverse transcription. *Biophys. J.*, **89**, 3470–3479.
59. Liu,H.W., Zeng,Y., Landes,C.F., Kim,Y.J., Zhu,Y., Ma,X., Vo,M.-N., Musier-Forsyth,K. and Barbara,P.F. (2007) Insights on the role of nucleic acid/protein interactions in chaperoned nucleic acid rearrangements of HIV-1 reverse transcription. *Proc. Natl Acad. Sci. USA*, **104**, 5261–5267.
60. Driscoll,M.D. and Hughes,S.H. (2000) Human immunodeficiency virus type 1 nucleocapsid protein can prevent self-priming of minus-strand strong stop DNA by promoting the annealing of short oligonucleotides to hairpin sequences. *J. Virol.*, **74**, 8785–8792.
61. Lanciault,C. and Champoux,J.J. (2005) Effects of unpaired nucleotides within HIV-1 genomic secondary structures on pausing and strand transfer. *J. Biol. Chem.*, **280**, 2413–2423.
62. Berkhout,B., van Wamel,J. and Klaver,B. (1995) Requirements for DNA strand transfer during reverse transcription in mutant HIV-1 virions. *J. Mol. Biol.*, **252**, 59–69.
63. Zhang,W.H., Hwang,C.K., Hu,W.-S., Gorelick,R.J. and Pathak,V.K. (2002) Zinc finger domain of murine leukemia virus nucleocapsid protein enhances the rate of viral DNA synthesis in vivo. *J. Virol.*, **76**, 7473–7484.
64. Derebail,S.S., Heath,M.J. and DeStefano,J.J. (2003) Evidence for the differential effects of nucleocapsid protein on strand transfer in various regions of the HIV genome. *J. Biol. Chem.*, **278**, 15702–15712.
65. Heath,M.J., Derebail,S.S., Gorelick,R.J. and DeStefano,J.J. (2003) Differing roles of the N- and C-terminal zinc fingers in human immunodeficiency virus nucleocapsid protein-enhanced nucleic acid annealing. *J. Biol. Chem.*, **278**, 30755–30763.
66. Moumen,A., Polomack,L., Unge,T., Véron,M., Buc,H. and Negroni,M. (2003) Evidence for a mechanism of recombination during reverse transcription dependent on the structure of the acceptor RNA. *J. Biol. Chem.*, **278**, 15973–15982.
67. Roda,R.H., Balakrishnan,M., Hanson,M.N., Wöhrl,B.M., Le Grice,S.F.J., Roques,B.P., Gorelick,R.J. and Bambara,R.A. (2003) Role of the reverse transcriptase, nucleocapsid protein, and template structure in the two-step transfer mechanism in retroviral recombination. *J. Biol. Chem.*, **278**, 31536–31546.
68. Derebail,S.S. and DeStefano,J.J. (2004) Mechanistic analysis of pause site-dependent and -independent recombinogenic strand transfer from structurally diverse regions of the HIV genome. *J. Biol. Chem.*, **279**, 47446–47454.

69. Galetto,R., Moumen,A., Giacomoni,V., Veron,M., Charneau,P. and Negroni,M. (2004) The structure of HIV-1 genomic RNA in the gp120 gene determines a recombination hot spot *in vivo*. *J. Biol. Chem.*, **279**, 36625–36632.
70. Galetto,R. and Negroni,M. (2005) Mechanistic features of recombination in HIV. *AIDS Rev.*, **7**, 92–102.
71. Hanson,M.N., Balakrishnan,M., Roques,B.P. and Bambara,R.A. (2005) Effects of donor and acceptor RNA structures on the mechanism of strand transfer by HIV-1 reverse transcriptase. *J. Mol. Biol.*, **353**, 772–787.
72. Heath,M.J. and Destefano,J.J. (2005) A complementary single-stranded docking site is required for enhancement of strand exchange by human immunodeficiency virus nucleocapsid protein on substrates that model viral recombination. *Biochemistry*, **44**, 3915–3925.
73. Galetto,R., Giacomoni,V., Véron,M. and Negroni,M. (2006) Dissection of a circumscribed recombination hot spot in HIV-1 after a single infectious cycle. *J. Biol. Chem.*, **281**, 2711–2720.
74. Song,M., Balakrishnan,M., Chen,Y., Roques,B.P. and Bambara,R.A. (2006) Stimulation of HIV-1 minus strand strong stop DNA transfer by genomic sequences 3' of the primer binding site. *J. Biol. Chem.*, **281**, 24227–24235.
75. Goldschmidt,V., Didierjean,J., Ehresmann,B., Ehresmann,C., Isel,C. and Marquet,R. (2006) Mg^{2+} dependency of HIV-1 reverse transcription, inhibition by nucleoside analogues and resistance. *Nucleic Acids Res.*, **34**, 42–52.
76. Guo,J., Wu,W., Yuan,Z.Y., Post,K., Crouch,R.J. and Levin,J.G. (1995) Defects in primer-template binding, processive DNA synthesis, and RNase H activity associated with chimeric reverse transcriptases having the murine leukemia virus polymerase domain joined to *Escherichia coli* RNase H. *Biochemistry*, **34**, 5018–5029.
77. Mathews,D.H., Sabina,J., Zuker,M. and Turner,D.H. (1999) Expanded sequence dependence of thermodynamic parameters improves prediction of RNA secondary structure. *J. Mol. Biol.*, **288**, 911–940.
78. Zuker,M., Mathews,D.H. and Turner,D.H. (1999) In Barciszewski,J. and Clark,B.F.C. (eds), *RNA Biochemistry and Biotechnology*. Kluwer Academic Publishers, Dordrecht, The Netherlands, pp. 11–43.
79. Zuker,M. (2003) Mfold web server for nucleic acid folding and hybridization prediction. *Nucleic Acids Res.*, **31**, 3406–3415.
80. Kim,C.-H. and Tinoco,I.Jr (2000) A retroviral RNA kissing complex containing only two G.C base pairs. *Proc. Natl Acad. Sci. USA*, **97**, 9396–9401.
81. Li,P.T., Bustamante,C. and Tinoco,I.Jr (2006) Unusual mechanical stability of a minimal RNA kissing complex. *Proc. Natl Acad. Sci. USA*, **103**, 15847–15852.
82. Dib-Hajj,F., Khan,R. and Giedroc,D.P. (1993) Retroviral nucleocapsid proteins possess potent nucleic acid strand renaturation activity. *Protein Sci.*, **2**, 231–243.